



Mechanical annealing and yielding transition in cyclically sheared binary glasses



Nikolai V. Priezjev ^{a,b}

^a Department of Mechanical and Materials Engineering, Wright State University, Dayton, OH 45435, United States

^b National Research University Higher School of Economics, Moscow 101000, Russia

ARTICLE INFO

Keywords:

Metallic glasses
Thermo-mechanical processing
Yielding transition
Oscillatory shear deformation
Molecular dynamics simulations

ABSTRACT

The effect of cyclic shear deformation on structural relaxation and yielding in binary glasses was examined using molecular dynamics simulations. We studied a binary mixture slowly cooled from the liquid phase to about half the glass transition temperature and then periodically deformed at small strain amplitudes during thousands of cycles. We found that the potential energy decays logarithmically upon increasing number of cycles. The analysis of nonaffine displacements revealed that the process of mechanical annealing proceeds via intermittent plastic rearrangements whose spatial extent decreases upon reaching lower energy states. We also probed the yielding behavior for glasses with different degrees of annealing by adjusting strain amplitude near the critical value. Interestingly, in contrast to zero-temperature amorphous solids, the critical strain amplitude remains unchanged for glasses with initially different energy levels. The formation of a shear band at the yielding transition correlates well with the sharp increase of the number of atoms with large nonaffine displacements.

1. Introduction

Understanding and controlling plastic deformation and relaxation in metallic glasses is important for biomedical, environmental and structural applications [1–4]. It is well established that plastic deformation in disordered solids is governed by swift irreversible rearrangements of small groups of atoms or shear transformations [5,6]. One of the challenges in widespread use of metallic glasses is their lack of ductility at a relaxed state and catastrophic failure via the formation of narrow regions called shear bands where strain is localized. In turn, a number of thermo-mechanical processing methods, such as high-pressure torsion, cold rolling, irradiation, and elastostatic loading, can be applied to rejuvenate metallic glasses and enhance their ductility [7]. It was recently discovered that cryogenic thermal cycling can rejuvenate metallic glasses due to internal stresses arising during spatially heterogeneous thermal expansion [8–20]. More recently, experiments and atomistic simulations showed that amorphous alloys can also be rejuvenated by quickly cooling across the glass transition under applied stress, so that a glass former freezes into a less relaxed structure [21,22]. Despite significant progress, however, modeling of process-structure-property relationships for metallic glasses with targeted properties remains a challenging task.

In recent years, the structural relaxation and yielding transition in

periodically deformed amorphous alloys were extensively studied using atomistic and continuum simulations [23–54]. The atomistic simulations are typically performed either in the athermal quasistatic limit where the energy is minimized after each incremental step or at finite temperatures and strain rates. The presence of thermal fluctuations becomes particularly important in two aspects of glassy dynamics; namely, the exact reversibility of atomic trajectories during steady-state deformation and near the yielding transition where there is an energy barrier for the formation of a shear band. It was originally shown using athermal quasistatic cyclic shear simulations that at sufficiently small strain amplitudes, disordered solids eventually evolve into periodic limit cycles where atoms follow the same trajectories for consecutive cycles [25,27]. By contrast, glassy systems under small-amplitude cyclic loading at finite temperatures continue exploring progressively lower energy states via sequential irreversible rearrangements of atoms [35, 37,38,43,52]. The mechanical annealing process can be further accelerated by alternating orientation of periodic shear deformation in two or three spatial dimensions [40,48]. Interestingly, it was recently demonstrated that the critical strain amplitude for yielding of zero-temperature disordered solids increases with the degree of annealing [44,47]. The same trend was reported for binary glasses at finite temperatures well below T_g , although an accurate determination of the critical strain amplitude is a challenging problem as it might take thousands of shear

E-mail address: nikolai.priezjev@wright.edu.

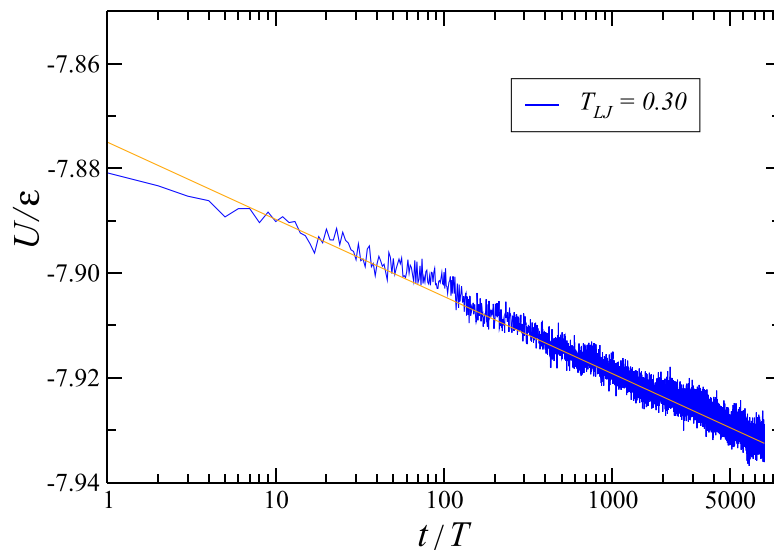


Fig. 1. (Color online) The variation of the potential energy at zero strain as a function of the number of shear cycles with the strain amplitude $\gamma_0 = 0.035$ at the temperature $T_{LJ} = 0.30 \epsilon/k_B$ and density $\rho = 1.2 \sigma^{-3}$. The period of oscillation is $T = 5000 \tau$. The straight line $y = -7.875 - 0.0064 \cdot \ln(t/T)$ is shown for reference.

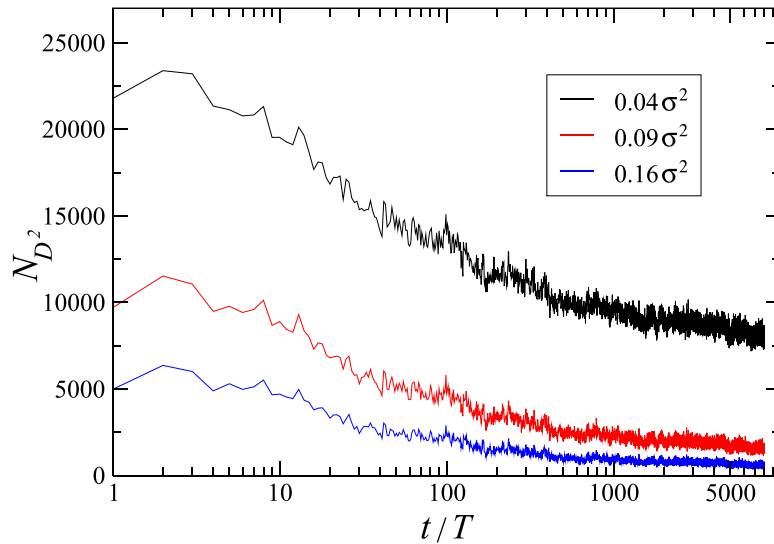


Fig. 2. (Color online) The number of atoms with large nonaffine displacements after one cycle as a function of the number of cycles with the strain amplitude $\gamma_0 = 0.035$ at $T_{LJ} = 0.30 \epsilon/k_B$ and $\rho = 1.2 \sigma^{-3}$. The nonaffine measure D^2 is greater than $0.04 \sigma^2$ (black curve), $0.09 \sigma^2$ (red curve), $0.16 \sigma^2$ (blue curve). The total number of atoms is $N_{tot} = 60000$. (For interpretation of the references to colour in this figure legend, the reader is referred to the web version of this article.)

cycles until the formation of a shear band, especially in large systems [46].

In this paper, molecular dynamics simulations are performed to study structural relaxation and yielding transition in binary glasses under oscillatory shear deformation. We consider stable glasses that are further relaxed via small-amplitude cyclic shear at the temperature not far below the glass transition temperature. It will be shown that the potential energy during the mechanical annealing process follows a logarithmic decay as a function of the number of loading cycles. The annealing process involves intermittent clusters of plastic rearrangements, whose typical size is gradually reduced upon reaching lower energy states. In addition, we investigate the yielding transition in glasses with different degrees of relaxation by varying strain amplitude near the critical value. Notably, we find that although the number of transient cycles until yielding increases, the critical strain amplitude remains the same upon increasing glass stability. These results are quantified and visualized via the spatiotemporal analysis of nonaffine

displacements.

This paper is structured as follows. The details of molecular dynamics simulations and periodic deformation protocol are described in the next section. The analysis of nonaffine displacements and potential energy during mechanical annealing and yielding transition is presented in Section 3. A brief summary of the results are given in the last section.

2. Molecular dynamics (MD) simulations

In this study, we used the binary (80:20) Lennard-Jones (LJ) mixture model, originally introduced by Kob and Andersen (KA) [55]. In the KA model, the interaction between different types of atoms is strongly non-additive, which suppresses crystallization upon cooling across the glass transition temperature [55]. Specifically, the interaction between atoms of types $\alpha, \beta = A, B$ is defined as follows:

$$V_{\alpha\beta}(r) = 4 \epsilon_{\alpha\beta} \left[\left(\frac{\sigma_{\alpha\beta}}{r} \right)^{12} - \left(\frac{\sigma_{\alpha\beta}}{r} \right)^6 \right], \quad (1)$$

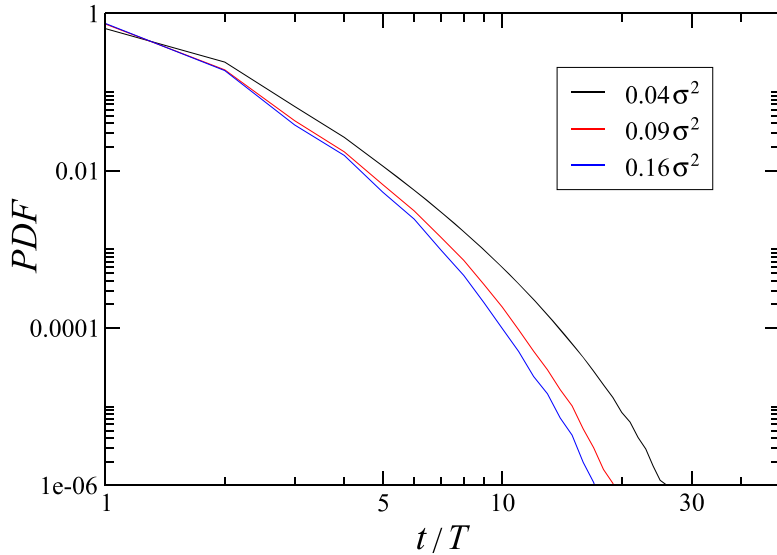


Fig. 3. (Color online) The normalized probability distribution function of the number of consecutive cycles with large nonaffine displacements. The oscillation period is $T = 5000 \tau$. The same deformation protocol as in Figs. 1 and 2. The nonaffine measure is $D^2 > 0.04 \sigma^2$ (black curve), $D^2 > 0.09 \sigma^2$ (red curve), $D^2 > 0.16 \sigma^2$ (blue curve). (For interpretation of the references to colour in this figure legend, the reader is referred to the web version of this article.)

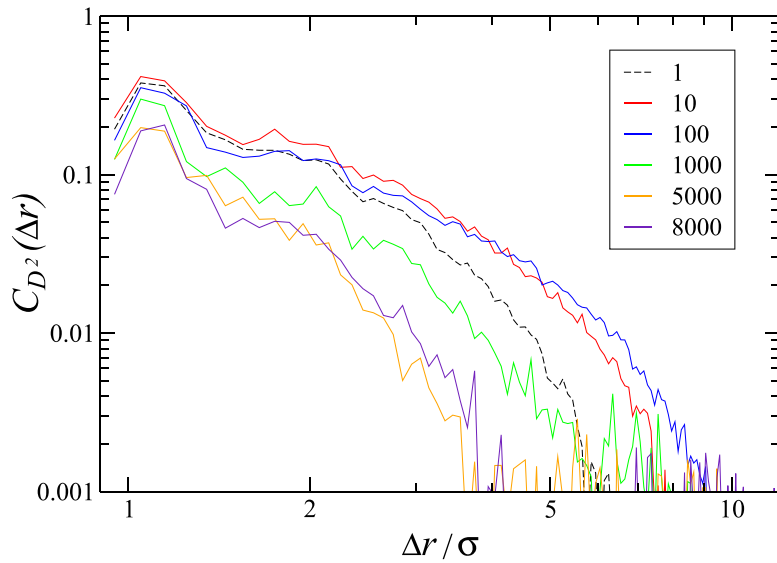


Fig. 4. (Color online) The correlation function $C_{D^2}(\Delta r)$ given by Eq. (4) for the indicated number of shear cycles with the strain amplitude $\gamma_0 = 0.035$ at $T_{LJ} = 0.30 \epsilon/k_B$ and $\rho = 1.2 \sigma^{-3}$. The nonaffine measure is evaluated for two configurations of atoms at zero strain during one full cycle with the period $T = 5000 \tau$.

where the model parameters are $\varepsilon_{AA} = 1.0$, $\varepsilon_{AB} = 1.5$, $\varepsilon_{BB} = 0.5$, $\sigma_{AA} = 1.0$, $\sigma_{AB} = 0.8$, $\sigma_{BB} = 0.88$, and $m_A = m_B$ [55]. The cutoff radius is $r_{c,\alpha\beta} = 2.5 \sigma_{\alpha\beta}$. This parametrization is similar to the one employed by Weber and Stillinger in order to study the amorphous metal-metalloid alloy Ni₈₀P₂₀ [56]. In the present study, the results are expressed in terms of the reduced units of length, mass, and energy, as follows: $\sigma = \sigma_{AA}$, $m = m_A$, and $\varepsilon = \varepsilon_{AA}$. In addition, the equations of motion for each atom were solved using the velocity Verlet algorithm with the time step $\Delta t_{MD} = 0.005 \tau$, where $\tau = \sigma\sqrt{m/\varepsilon}$ is the LJ time [57,58].

The binary glass was prepared as follows. We first placed the binary mixture of 60 000 atoms in a periodic box of size $L = 36.84 \sigma$ and equilibrated the liquid phase at $T_{LJ} = 1.0 \epsilon/k_B$ and density $\rho = \rho_A + \rho_B = 1.2 \sigma^{-3}$. Here, k_B is the Boltzmann constant. To remind, the critical temperature of the KA model at $\rho = 1.2 \sigma^{-3}$ is $T_g = 0.435 \epsilon/k_B$ [55]. In our simulations, the system temperature was regulated via the Nosé-Hoover thermostat [57,58]. Next, we reduced the system

temperature from $T_{LJ} = 1.0 \epsilon/k_B$ to $0.3 \epsilon/k_B$ with the rate of $10^{-5} \epsilon/k_B \tau$ at constant density $\rho = 1.2 \sigma^{-3}$. After thermal annealing, the binary glass was subjected to cyclic shear deformation along the xz plane, as follows:

$$\gamma_{xz}(t) = \gamma_0 \sin(2\pi t / T), \quad (2)$$

where the oscillation period and frequency are $T = 5000 \tau$ and $\omega = 2\pi/T = 1.26 \times 10^{-3} \tau^{-1}$, respectively. To avoid confusion, the oscillation period is denoted by T , whereas the system temperature is indicated by T_{LJ} . The system was loaded during 8000 shear cycles with the strain amplitude $\gamma_0 = 0.035$ at the temperature $T_{LJ} = 0.30 \epsilon/k_B$ and density $\rho = 1.2 \sigma^{-3}$. Due to computational limitations, the simulations were carried out only for one sample and it took about 220 days using 40 processors in parallel. In addition, the yielding transition was probed in annealed samples after 1000 and 5000 shear cycles with $\gamma_0 = 0.035$ by applying cyclic shear along the xz plane with strain amplitudes in the range $0.035 \leq \gamma_0 \leq 0.043$.

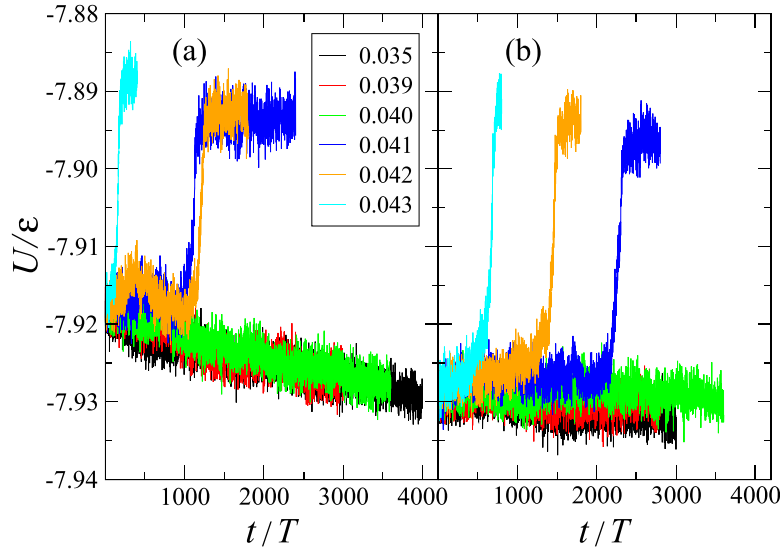


Fig. 5. (Color online) The variation of the potential energy, U/ϵ , for binary glasses that were initially annealed during (a) 1000 and (b) 5000 shear cycles with the strain amplitude $\gamma_0 = 0.035$ at $T_{LJ} = 0.30 \epsilon/k_B$ and $\rho = 1.2 \sigma^{-3}$. Each curve represents the potential energy after a full cycle at zero strain. The values of strain amplitudes are tabulated in the inset. The oscillation period is $T = 5000 \tau$.

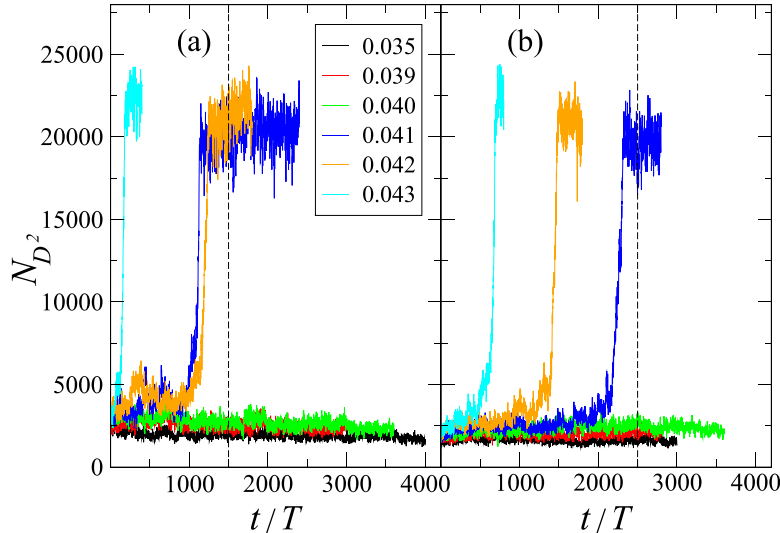


Fig. 6. (Color online) The number of atoms with nonaffine displacements after a full cycle $D^2 > 0.09 \sigma^2$ for the indicated values of the strain amplitude. The glass was initially deformed for (a) 1000 and (b) 5000 shear cycles with the strain amplitude $\gamma_0 = 0.035$ at $T_{LJ} = 0.30 \epsilon/k_B$ and $\rho = 1.2 \sigma^{-3}$. The same deformation protocols as in Fig. 5. The vertical dashed lines indicate the number of cycles used to load binary glasses shown in Figs. 7 and 8.

3. Results

It has been long realized that a wide range of energy states in metallic glasses can be accessed by using various thermal and mechanical processing methods [7]. Among simple processing routes, a slow cooling across the glass transition temperature that results in low energy, stable glasses. In addition, it was shown that glasses can be further annealed via cyclic loading with strain amplitudes below a critical value [24,35, 44,59]. By contrast, upon increasing strain amplitude of periodic deformation, metallic glasses undergo yielding transition via formation of shear bands in sufficiently large systems [32,33]. While the effect of glass stability on yielding transition in zero-temperature amorphous solids was recently clarified [44,47], the influence of thermal fluctuations on the critical strain amplitude for stable glasses requires further investigation.

In the present study, we considered relatively stable glasses that were initially prepared by cooling across the glass transition temperature with

a computationally slow rate of $10^{-5} \epsilon/k_B \tau$, and then further relaxed via small-amplitude cyclic loading. All simulations were carried out at an intermediate temperature $T_{LJ} = 0.30 \epsilon/k_B$ not far below the glass transition temperature $T_g = 0.435 \epsilon/k_B$. The variation of the potential energy at the end of each cycle when strain is zero is shown in Fig. 1 for 8000 cycles with the strain amplitude $\gamma_0 = 0.035$. As is evident, the relaxation process during mechanical annealing follows the logarithmic decay (see the orange curve in Fig. 1). In the previous studies on the KA glasses, it was shown that relaxation is enhanced when the glass is periodically deformed with the strain amplitude $\gamma_0 = 0.035$ at the temperature $T_{LJ} = 0.30 \epsilon/k_B$ and density $\rho = 1.2 \sigma^{-3}$ [37,52]. Moreover, upon subsequent cooling the glass to a very low temperature $T_{LJ} = 0.01 \epsilon/k_B$, it was found that the potential energy of inherent structures also follows a logarithmic decay as a function of the number of loading cycles [52].

In practice, the local plastic deformation in disordered solids can be detected by analyzing the so-called nonaffine displacements of atoms

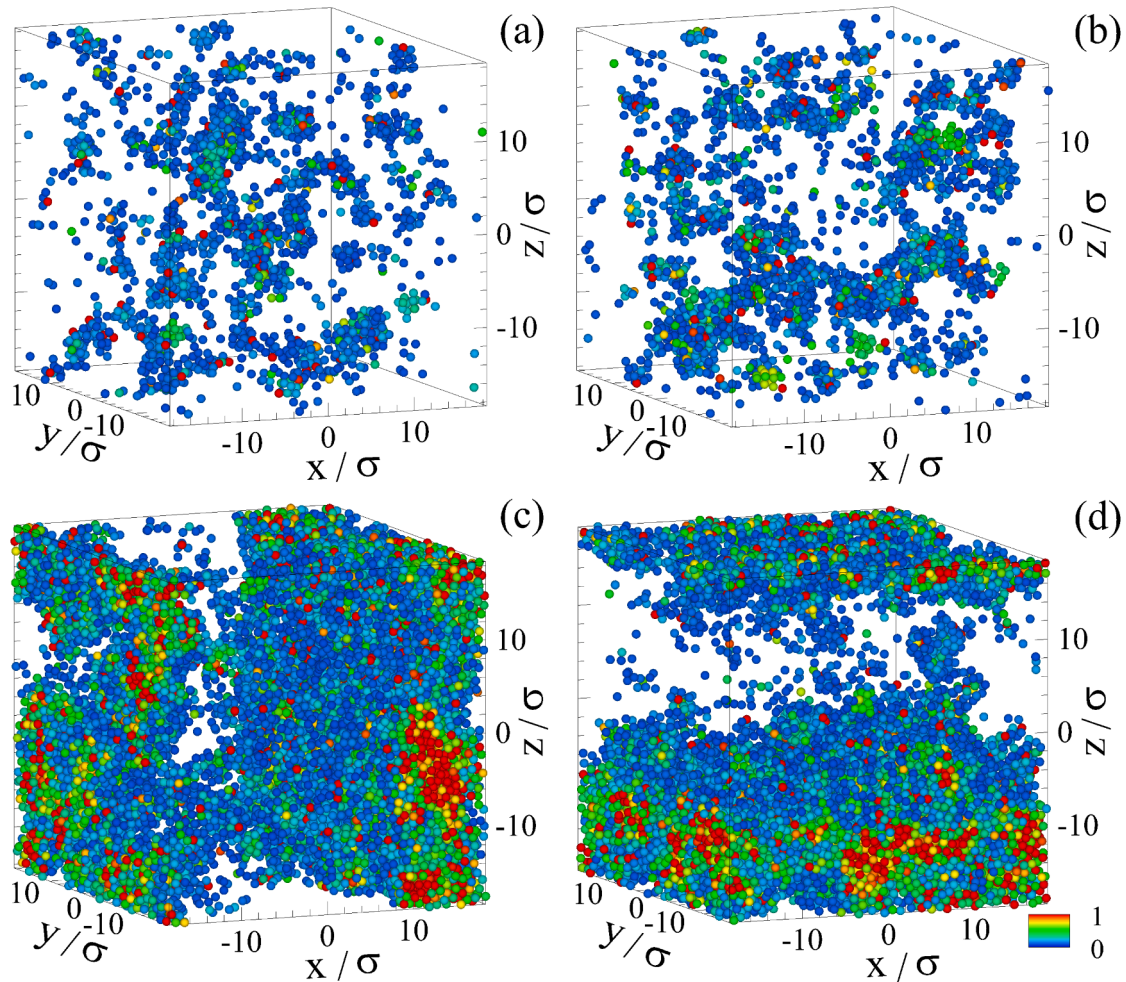


Fig. 7. (Color online) The spatial configurations of atoms with large nonaffine displacements [$D^2(1499 T, T) > 0.09 \sigma^2$] during one shear cycle with the oscillation period $T = 5000 \tau$. The glass was initially loaded for 1000 cycles with $\gamma_0 = 0.035$ and then periodically deformed for additional 1500 cycles with (a) $\gamma_0 = 0.035$, (b) $\gamma_0 = 0.040$, (c) $\gamma_0 = 0.041$, and (d) $\gamma_0 = 0.042$. The magnitude of D^2 for each atom is indicated by the legend color. The same loading protocol as in Figs. 5 (a) and 6 (a).

with respect to their neighbors [60]. More specifically, the nonaffine measure D^2 for the i -th atom is computed using the matrix J_i , which linearly transforms a group of neighbors and simultaneously minimizes the following equation:

$$D^2(t, \Delta t) = \frac{1}{N_i} \sum_{j=1}^{N_i} \left\{ \mathbf{r}_j(t + \Delta t) - \mathbf{r}_i(t + \Delta t) - J_i \left[\mathbf{r}_j(t) - \mathbf{r}_i(t) \right] \right\}^2, \quad (3)$$

where the summation is carried over N_i neighboring atoms within 1.5σ from the position vector $\mathbf{r}_i(t)$, and Δt in the time difference between two instantaneous configurations of atoms. The local plastic rearrangement during the time interval Δt is typically associated with the cage breaking event. In other words, an atom i escapes from a cage of its neighbors when its nonaffine displacement becomes greater than about 0.1σ for the KA binary glass [29]. Among other types of deformation, large-amplitude oscillatory shear was shown to induce collective nonaffine displacements in binary glasses ranging from small clusters to shear bands upon increasing strain amplitude above the critical value [33].

The gradual decrease in potential energy due to small-amplitude cyclic loading shown in Fig. 1 occurs via a sequence of local plastic events. The total number of atoms with relatively large nonaffine displacements during one cycle is shown in Fig. 2 as a function of the cycle number. In this analysis, the nonaffine displacements were computed for

two consecutive configurations of atoms at zero strain and the time interval $\Delta t = T$. For comparison, the number of atoms with the nonaffine measure D^2 in Eq. (3) greater than $0.04\sigma^2$, $0.09\sigma^2$ and $0.16\sigma^2$ are reported in Fig. 2. It can be seen that during the first 10 cycles about one third of the total number of atoms (≈ 20000) undergo large nonaffine displacements ($D^2 > 0.04\sigma^2$), and the number, N_{D^2} , monotonically decreases (to ≈ 8000) as the system explores progressively lower energy states upon cyclic loading. It should be commented that a large value of $D^2 > 0.04\sigma^2$ during one cycle does not necessarily involve an irreversible rearrangement, since an atom can return back to the cage of its neighbors after a few cycles [29]. However, the larger the value of D^2 , the higher the probability of irreversible displacement and, therefore, local structural relaxation [29]. As shown in Fig. 2, the number of atoms with larger thresholds, $D^2 > 0.09\sigma^2$ and $0.16\sigma^2$, is significantly reduced during 8000 cycles, indicating a gradual approach towards reversible deformation. Note also that the function $N_{D^2}(t/T)$ reported in Fig. 2 does not follow the logarithmic decay shown for the potential energy in Fig. 1.

The spatiotemporal distribution of plastic events during the mechanical annealing process includes the formation of intermittent clusters of atoms with large nonaffine displacements [23,35]. In the present study, we computed the number of consecutive cycles, during which the nonaffine measure after each cycle remained above a certain threshold. The data were averaged over $N_{tot} = 60\,000$ atoms and 8000 shear cycles.

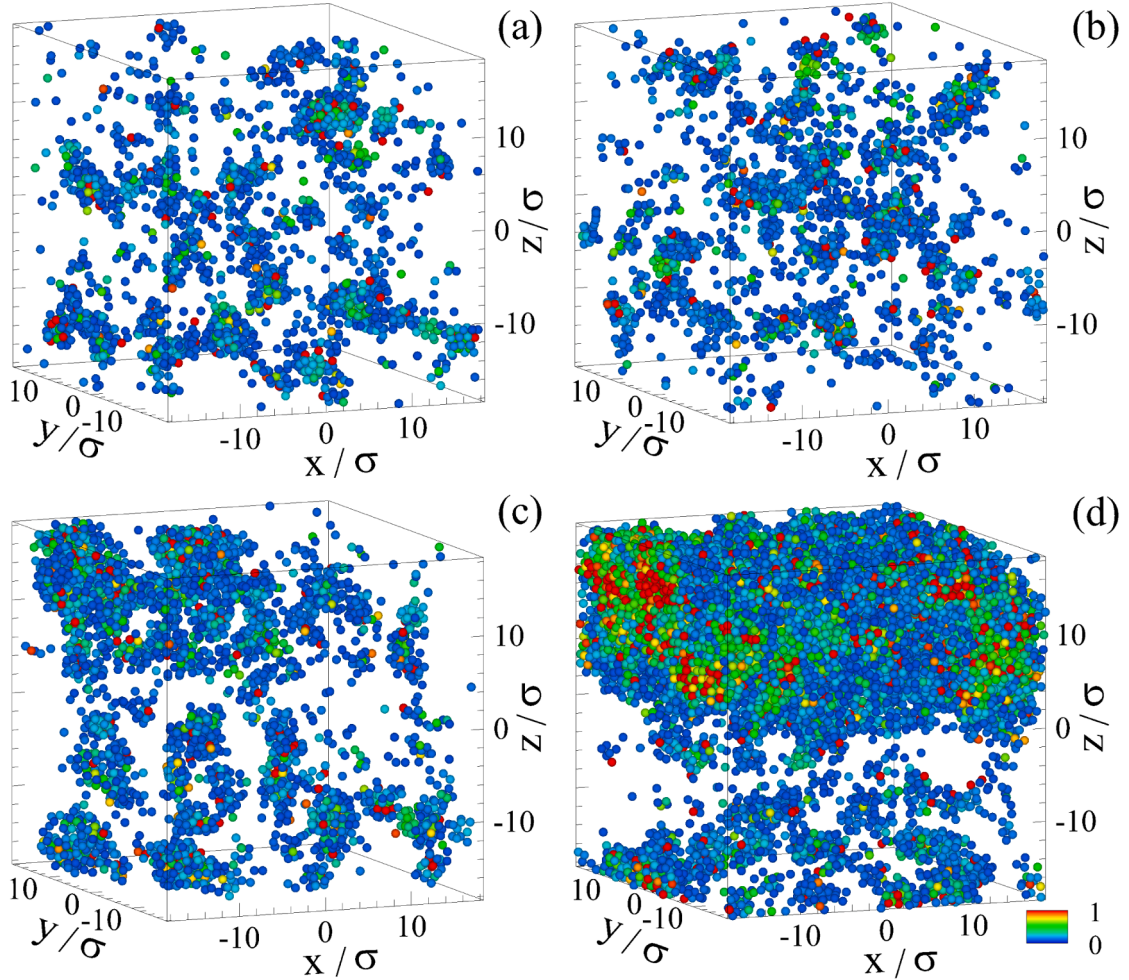


Fig. 8. (Color online) The instantaneous snapshots of atoms with the nonaffine measure $D^2(2499 T, T) > 0.09 \sigma^2$ during one shear cycle with the period $T = 5000 \tau$. The binary glass was first loaded for 5000 cycles with the strain amplitude $\gamma_0 = 0.035$ and then periodically deformed for additional 2500 cycles with (a) $\gamma_0 = 0.035$, (b) $\gamma_0 = 0.039$, (c) $\gamma_0 = 0.040$, and (d) $\gamma_0 = 0.041$. The legend color indicates the magnitude of the nonaffine measure. The same deformation protocol as in Figs. 5 (b) and 6 (b).

The normalized probability distribution function for the number of consecutive cycles is plotted in Fig. 3 for the nonaffine measure D^2 greater than $0.04 \sigma^2$, $0.09 \sigma^2$ and $0.16 \sigma^2$. It can be seen that the distribution functions quickly decay upon increasing number of cycles, while, not surprisingly, the probability of repeated plastic rearrangements is slightly higher when $D^2 > 0.04 \sigma^2$. These results demonstrate that most of the atoms undergo large nonaffine displacements during one or two cycles, although at the beginning of the cyclic loading process, there is a finite probability of irreversible displacements over ten consecutive cycles.

The spatial extent of fluctuations of nonaffine displacements can be quantified via the normalized, equal-time correlation function [61], as follows:

$$C_{D^2}(\Delta \mathbf{r}) = \frac{\langle D^2(\mathbf{r} + \Delta \mathbf{r}) D^2(\mathbf{r}) \rangle - \langle D^2(\mathbf{r}) \rangle^2}{\langle D^2(\mathbf{r})^2 \rangle - \langle D^2(\mathbf{r}) \rangle^2}, \quad (4)$$

where the brackets $\langle \cdot \rangle$ denote averaging over all pairs of atoms, and the nonaffine measure is computed for two atomic configurations at zero strain separated by $\Delta t = T$. The correlation function $C_{D^2}(\Delta \mathbf{r})$ was computed for two consecutive configurations after a certain number of shear cycles with the strain amplitude $\gamma_0 = 0.035$ at $T_{LJ} = 0.30 \epsilon/k_B$ and $\rho = 1.2 \sigma^{-3}$. The results are shown in Fig. 4 for the indicated number of shear cycles. Although the data are somewhat noisy, it can be clearly

seen that with increasing number of cycles, the spatial correlations become more short-ranged, implying smaller size of plastic events in better annealed glasses. The exception from this trend is the correlation function computed after the first cycle, which might be related to a relatively stable configuration after thermal annealing that precedes cyclic loading. Notice in Fig. 2 that the number of atoms with large nonaffine displacements has a maximum after the second cycle.

We next probed the yielding behavior in binary glasses with different degrees of relaxation. During the mechanical annealing process shown in Fig. 1, two samples were saved after 1000 and 5000 cycles with the strain amplitude $\gamma_0 = 0.035$ at $T_{LJ} = 0.30 \epsilon/k_B$ and $\rho = 1.2 \sigma^{-3}$. Then, these samples were periodically sheared along the xz plane with strain amplitudes in the range $0.035 \leq \gamma_0 \leq 0.043$. The variation of the potential energy as a function of the cycle number for both samples is shown in Fig. 5. Remarkably, it can be seen that although initially the potential energy is different, the critical strain amplitude $\gamma_0 = 0.040$ remains unchanged. Note that the less relaxed sample in Fig. 5 (a) becomes better annealed upon cyclic loading at strain amplitudes $0.035 \leq \gamma_0 \leq 0.040$, whereas the yielding transition at $\gamma_0 = 0.041$ is delayed by about 2000 cycles for the more relaxed glass, as shown in Fig. 5 (b). Moreover, the potential energy curves for the strain amplitudes $\gamma_0 \leq 0.040$ in Fig. 5 are essentially the same, which implies that the logarithmic dependence of the potential energy as a function of the cycle number reported in Fig. 1 holds in the range of strain amplitudes $0.035 \leq \gamma_0 \leq 0.040$ below the

critical value.

It should be emphasized that the results of athermal quasistatic cyclic shear simulations showed that the critical strain amplitude and the discontinuous energy change at the yielding transition increase in more stable glasses [44,47]. Note that in athermal systems, the trajectories of all atoms become exactly reversible after a number of transient cycles, and the potential energy of reversible states is nearly independent of the strain amplitude for sufficiently well annealed glasses [44,47]. Similar conclusions were reached for stable glasses at the finite temperature $T_{LJ} = 0.01 \epsilon/k_B \ll T_g$, although precise determination of the critical strain amplitude was computationally challenging, since the system dynamics remained nearly reversible during thousands of cycles, leaving the possibility of yielding under continued loading [46]. Therefore, the results at the intermediate temperature $T_{LJ} = 0.30 \epsilon/k_B$ presented in Fig. 5 are qualitatively different from the zero- and low-temperature cases, as they indicate that with increasing glass stability, the number of cycles until yielding increases but the critical strain amplitude remains unchanged.

The processes of structural relaxation and yielding are reflected in the distribution of nonaffine displacements. Fig. 6 shows the number of atoms with large nonaffine displacements during one cycle, $D^2 > 0.09 \sigma^2$, for the same deformation protocols as in Fig. 5. It can be observed that the yielding transition in each case is associated with an abrupt increase in the number of atoms involved in plastic deformation. Note also that, somewhat unexpectedly, the yielding transition for the strain amplitude $\gamma_0 = 0.042$ is delayed with respect to loading at a smaller strain amplitude $\gamma_0 = 0.041$ [see Fig. 6 (a)], which correlates well with the results for the potential energy reported in Fig. 5 (a). Moreover, the plateaus in N_{D^2} after yielding at strain amplitudes $0.041 \leq \gamma_0 \leq 0.043$ (see Fig. 6) correspond to plastic deformation within shear bands formed across the whole sample.

In order to visualize the spatial distribution of plastic events, we plotted snapshots of atomic configurations after 1500 and 2500 cycles (see the vertical dashed lines in Fig. 6) in Figs. 7 and 8, respectively. For clarity, atoms with the nonaffine measure $D^2 < 0.09 \sigma^2$ are not displayed. Notice the appearance of multiple clusters during the relaxation process at strain amplitudes $\gamma_0 = 0.035$ and 0.040 in Fig. 7 (a-b), whereas shear bands are formed along different planes after yielding at higher strain amplitudes $\gamma_0 = 0.041$ and 0.042 , as shown in Fig. 7 (c-d). During the mechanical annealing process shown in Fig. 6 (b), the clusters of atoms with $D^2 > 0.09 \sigma^2$ remain finite but their size becomes larger upon increasing strain amplitude, i.e., $\gamma_0 = 0.035, 0.039$, and 0.040 [see Fig. 8 (a-c)]. We also comment that shear bands in Figs. 7 (c-d) and 8 (d) have approximately the same width, which is consistent with the plateau levels in N_{D^2} after yielding transitions reported in Fig. 6. Altogether, these results indicate that structural relaxation and yielding in binary glasses under cyclic shear correlate well with the local plastic activity expressed in terms of the number of atoms with large nonaffine displacements.

4. Conclusions

In summary, we investigated the effect of cyclic shear deformation on structural relaxation and yielding behavior in binary glasses using molecular dynamics simulations. We considered a model glass former that consists of a binary mixture of atoms with strongly non-additive interactions, which suppresses crystallization upon cooling below the glass transition temperature. The stable glass was prepared by slowly cooling across the glass transition to an intermediate temperature not far below T_g . We found that upon small-amplitude cyclic loading, the potential energy per atom follows a logarithmic decay as a function of the number of cycles. This mechanical annealing process is associated with intermittent plastic rearrangements, whose typical size reduces as the system is relocated to progressively lower energy states upon cyclic loading.

Furthermore, the yielding behavior was probed in glasses with different degrees of stability by applying cyclic shear deformation with strain amplitudes near the critical value. The yielding transition and the formation of system-spanning shear bands were quantified and visualized via the analysis of nonaffine displacements. Remarkably, the results of numerical simulations indicate that the critical strain amplitude remains unchanged for more relaxed glasses at the intermediate temperature. This is in contrast to previous results of the same model glass at temperatures well below T_g , where it was reported that the critical strain amplitude is larger for more stable glasses [46,52].

Declaration of Competing Interest

The authors declare that they have no known competing financial interests or personal relationships that could have appeared to influence the work reported in this paper.

Acknowledgments

Financial support from the National Science Foundation (CNS-1531923) is gratefully acknowledged. Molecular dynamics simulations were carried out at Wright State University's Computing Facility and the Ohio Supercomputer Center using the LAMMPS code developed at Sandia National Laboratories [57].

References

- [1] T. Egami, T. Iwashita, W. Dmowski, Mechanical properties of metallic glasses, *Metals* 3 (2013) 77.
- [2] J.C. Qiao, Q. Wang, J.M. Pelletier, H. Kato, R. Casalini, D. Crespo, E. Pineda, Y. Yao, Y. Yang, Structural heterogeneities and mechanical behavior of amorphous alloys, *Prog. Mater. Sci.* 104 (2019) 250.
- [3] S.T. Rajan, A. Arockiarajan, Thin film metallic glasses for bioimplants and surgical tools: a review, *J. Alloys Compd.* 876 (2021) 159939.
- [4] N. Sohrabi, J. Jhabvala, R.E. Logue, Additive manufacturing of bulk metallic glasses—process, challenges and properties: a review, *Metals* 11 (2021) 1279.
- [5] F. Spaepen, A microscopic mechanism for steady state inhomogeneous flow in metallic glasses, *Acta Metall.* 25 (1977) 407.
- [6] A.S. Argon, Plastic deformation in metallic glasses, *Acta Metall.* 27 (1979) 47.
- [7] Y. Sun, A. Concstell, A.L. Greer, Thermomechanical processing of metallic glasses: extending the range of the glassy state, *Nat. Rev. Mater.* 1 (2016) 16039.
- [8] S.V. Ketov, Y.H. Sun, S. Nachum, Z. Lu, A. Chechli, A.R. Bernalin, H.Y. Bai, W. Wang, D.V. Louzguine-Luzgin, M.A. Carpenter, A.L. Greer, Rejuvenation of metallic glasses by non-affine thermal strain, *Nature* 524 (2015) 200.
- [9] W. Guo, J. Saidi, M. Zhao, S. Lu, S. Wu, Rejuvenation of zr-based bulk metallic glass matrix composite upon deep cryogenic cycling, *Mater. Lett.* 247 (2019) 135.
- [10] N.V. Priezjev, The effect of cryogenic thermal cycling on aging, rejuvenation, and mechanical properties of metallic glasses, *J. Non-Cryst. Solids* 503 (2019) 131.
- [11] Q.-L. Liu, N.V. Priezjev, The influence of complex thermal treatment on mechanical properties of amorphous materials, *Comput. Mater. Sci.* 161 (2019) 93.
- [12] N.V. Priezjev, Potential energy states and mechanical properties of thermally cycled binary glasses, *J. Mater. Res.* 34 (2019) 2664.
- [13] M. Samavatian, R. Gholamipour, A.A. Amadeh, S. Mirdamadi, Correlation between plasticity and atomic structure evolution of a rejuvenened bulk metallic glass, *Metall. Mater. Trans. A* 50 (2019) 4743.
- [14] N.V. Priezjev, Atomistic modeling of heat treatment processes for tuning the mechanical properties of disordered solids, *J. Non-Cryst. Solids* 518 (2019) 128.
- [15] J. Ketkaew, R. Yamada, H. Wang, D. Kuldinow, B.S. Schroers, W. Dmowski, T. Egami, J. Schroers, The effect of thermal cycling on the fracture toughness of metallic glasses, *Acta Mater.* 184 (2020) 100.
- [16] C.M. Meylan, F. Papparotto, S. Nachum, J. Orava, M. Miglierini, V. Basykh, J. Ferenc, T. Kulik, A.L. Greer, Stimulation of shear-transformation zones in metallic glasses by cryogenic thermal cycling, *J. Non-Cryst. Solids* 584 (2020) 120299.
- [17] W. Zhang, Q.C. Xiang, C.Y. Ma, Y.L. Ren, K.Q. Qiu, Relaxation-to-rejuvenation transition of a ce-based metallic glass by quenching/cryogenic treatment performed at sub-tg, *J. Alloys Compd.* 825 (2020) 153997.
- [18] T. Tjahjono, M. Elveny, S. Chupradit, D. Bokov, H.T. Hoi, M. Pandey, Role of cryogenic cycling rejuvenation on flow behavior of zr cu al ni ag metallic glass at relaxation temperature, *Trans. Indian Inst. Met.* 74 (2021) 3241.
- [19] B. Shang, W. Wang, A.L. Greer, P. Guan, Atomistic modelling of thermal-cycling rejuvenation in metallic glasses, *Acta Mater.* 213 (2021) 116952.
- [20] M. Bruns, F. Varnik, Rejuvenation in deep thermal cycling of a generic model glass: A study of per-particle energy distribution, *Materials* 15 (2022) 829.
- [21] R.M.O. Mota, E.T. Lund, S. Sohn, D.J. Browne, D.C. Hofmann, S. Curtarolo, A. van de Walle, J. Schroers, Enhancing ductility in bulk metallic glasses by straining during cooling, *Commun. Mater.* 2 (2021) 23.

- [22] N.V. Priezjev, Cooling under applied stress rejuvenates amorphous alloys and enhances their ductility, *Metals* 11 (2021) 67.
- [23] N.V. Priezjev, Heterogeneous relaxation dynamics in amorphous materials under cyclic loading, *Phys. Rev. E* 87 (2013) 052302.
- [24] D. Fiocco, G. Foffi, S. Sastry, Oscillatory athermal quasistatic deformation of a model glass, *Phys. Rev. E* 88 (R) (2013) 020301.
- [25] I. Regev, T. Lookman, C. Reichhardt, Onset of irreversibility and chaos in amorphous solids under periodic shear, *Phys. Rev. E* 88 (2013) 062401.
- [26] N. Perchikov, E. Bouchbinder, Variable-amplitude oscillatory shear response of amorphous materials, *Phys. Rev. E* 89 (2014) 062307.
- [27] I. Regev, J. Weber, C. Reichhardt, K.A. Dahmen, T. Lookman, Reversibility and criticality in amorphous solids, *Nat. Commun.* 6 (2015) 8805.
- [28] Y.F. Ye, S. Wang, J. Fan, C.T. Liu, Y. Yang, Atomistic mechanism of elastic softening in metallic glass under cyclic loading revealed by molecular dynamics simulations, *Intermetallics* 68 (2016) 5.
- [29] N.V. Priezjev, Reversible plastic events during oscillatory deformation of amorphous solids, *Phys. Rev. E* 93 (2016) 013001.
- [30] T. Kawasaki, L. Berthier, Macroscopic yielding in jammed solids is accompanied by a non-equilibrium first-order transition in particle trajectories, *Phys. Rev. E* 94 (2016) 022615.
- [31] N.V. Priezjev, Nonaffine rearrangements of atoms in deformed and quiescent binary glasses, *Phys. Rev. E* 94 (2016) 023004.
- [32] P. Leishangthem, A.D.S. Parmar, S. Sastry, The yielding transition in amorphous solids under oscillatory shear deformation, *Nat. Commun.* 8 (2017) 14653.
- [33] N.V. Priezjev, Collective nonaffine displacements in amorphous materials during large-amplitude oscillatory shear, *Phys. Rev. E* 95 (2017) 023002.
- [34] M. Fan, M. Wang, K. Zhang, Y. Liu, J. Schroers, M.D. Shattuck, C.S. O'Hern, The effects of cooling rate on particle rearrangement statistics: rapidly cooled glasses are more ductile and less reversible, *Phys. Rev. E* 95 (2017) 022611.
- [35] N.V. Priezjev, Molecular dynamics simulations of the mechanical annealing process in metallic glasses: effects of strain amplitude and temperature, *J. Non-Cryst. Solids* 479 (2018) 42.
- [36] N.V. Priezjev, The yielding transition in periodically sheared binary glasses at finite temperature, *Comput. Mater. Sci.* 150 (2018) 162.
- [37] P. Das, A.D.S. Parmar, S. Sastry, Annealing glasses by cyclic shear deformation, arXiv:1805.12476 (2018).
- [38] N.V. Priezjev, Slow relaxation dynamics in binary glasses during stress-controlled, tension-compression cyclic loading, *Comput. Mater. Sci.* 153 (2018) 235.
- [39] A.D.S. Parmar, S. Kumar, S. Sastry, Strain localization above the yielding point in cyclically deformed glasses, *Phys. Rev. X* 9 (2019) 021018.
- [40] N.V. Priezjev, Accelerated relaxation in disordered solids under cyclic loading with alternating shear orientation, *J. Non-Cryst. Solids* 525 (2019) 119683.
- [41] S. Li, P. Huang, F. Wang, Rejuvenation saturation upon cyclic elastic loading in metallic glass, *Comput. Mater. Sci.* 166 (2019) 318.
- [42] N.V. Priezjev, Shear band formation in amorphous materials under oscillatory shear deformation, *Metals* 10 (2020) 300.
- [43] P.K. Jana, N.V. Priezjev, Structural relaxation in amorphous materials under cyclic tension-compression loading, *J. Non-Cryst. Solids* 540 (2020) 120098.
- [44] W.T. Yeh, M. Ozawa, K. Miyazaki, T. Kawasaki, L. Berthier, Glass stability changes the nature of yielding under oscillatory shear, *Phys. Rev. Lett.* 124 (2020) 225502.
- [45] N.V. Priezjev, Alternating shear orientation during cyclic loading facilitates yielding in amorphous materials, *J. Mater. Eng. Perform.* 29 (2020) 7328.
- [46] N.V. Priezjev, A delayed yielding transition in mechanically annealed binary glasses at finite temperature, *J. Non-Cryst. Solids* 548 (2020) 120324.
- [47] H. Bhaumik, G. Foffi, S. Sastry, The role of annealing in determining the yielding behavior of glasses under cyclic shear deformation, *PNAS* 118 (2021) 2100227118.
- [48] V.V. Krishnan, K. Ramola, S. Karmakar, Annealing effects of multidirectional oscillatory shear in model glass formers, arXiv:2112.07412 (2021).
- [49] N.V. Priezjev, Accessing a broader range of energy states in metallic glasses by variable-amplitude oscillatory shear, *J. Non-Cryst. Solids* 560 (2021) 120746.
- [50] K. Khirallah, B. Tyukodi, D. Vandembroucq, C.E. Maloney, Yielding in an integer automaton model for amorphous solids under cyclic shear, *Phys. Rev. Lett.* 126 (2021) 218005.
- [51] N.V. Priezjev, Shear band healing in amorphous materials by small-amplitude oscillatory shear deformation, *J. Non-Cryst. Solids* 566 (2021) 120874.
- [52] N.V. Priezjev, Yielding transition in stable glasses periodically deformed at finite temperature, *Comput. Mater. Sci.* 200 (2021) 110831.
- [53] C. Liu, E.E. Ferrero, E.A. Jagla, K. Martens, A. Rosso, L. Talon, The fate of shear-oscillated amorphous solids, *J. Chem. Phys.* 156 (2022) 104902.
- [54] S. Mitra, S. Marin-Aguilar, S. Sastry, F. Smalleenburg, G. Foffi, Correlation between plastic rearrangements and local structure in a cyclically driven glass, *J. Chem. Phys.* 156 (2022) 074503.
- [55] W. Kob, H.C. Andersen, Testing mode-coupling theory for a supercooled binary lennard-jones mixture: the van hove correlation function, *Phys. Rev. E* 51 (1995) 4626.
- [56] T.A. Weber, F.H. Stillinger, Local order and structural transitions in amorphous metal-metalloid alloys, *Phys. Rev. B* 31 (1985) 1954.
- [57] S.J. Plimpton, Fast parallel algorithms for short-range molecular dynamics, *J. Comp. Phys.* 117 (1995) 1.
- [58] M.P. Allen, D.J. Tildesley, Computer simulation of liquids, Clarendon, Oxford, 1987.
- [59] D.J. Lacks, M.J. Osborne, Energy landscape picture of overaging and rejuvenation in a sheared glass, *Phys. Rev. Lett.* 93 (2004) 255501.
- [60] M.L. Falk, J.S. Langer, Dynamics of viscoplastic deformation in amorphous solids, *Phys. Rev. E* 57 (1998) 7192.
- [61] V. Chikkadi, P. Schall, Nonaffine measures of particle displacements in sheared colloidal glasses, *Phys. Rev. E* 85 (2012) 031402.